Haberman et al., Supplemental material for "*Prominent hippocampal CA3 gene expression profile in neurocognitive aging"*

Supplemental Text

Methods

Behavioral characterization: Behavioral assessment of memory function in a Morris water maze task, was conducted as previously described (Gallagher et al., 1993). Briefly, the water maze consisted of a circular pool surrounded by white curtains with black patterns affixed to provide a configuration of spatial cues. The rats were trained for eight days (three trials per day) to locate a camouflaged escape platform that remained at the same location throughout training. Every sixth trial consisted of a probe trial (free swim with no escape platform) that served to assess the development of a spatially localized search for the escape platform. During these probe trials, a learning index was generated from the proximity of the rat to the escape platform and was used to define impairment in the rats. The learning index is the sum of weighted proximity scores obtained during probe trials, with low scores reflecting searches near the escape platform and high scores reflecting searches farther away from the platform (Gallagher et al., 1993). Aged rats performing within the range of young are designated aged unimpaired (AU) whereas those performing worse than young are considered aged impaired (AI). Cue training

(visible escape platform) occurred on the last day of training to test for sensorimotor and motivational factors independent of spatial learning.

Hippocampal Dissection: 26 rats (16 aged, 10 young) were sacrificed two weeks after completion of all behavioral testing by rapid decapitation, and brains removed from the skull. Brains were then chilled in ice cold PBS and all further manipulations performed on a cold plate. Whole hippocampi were dissected out and 400 μm sections were sliced throughout the entire rostral-caudal extent of the hippocampus. The CA1, CA3 and dentate gyrus were microdissected by hand under a dissecting microscope. Sub-regional boundaries were clearly visible under these conditions. Tissue for each region was pooled across hemispheres of the same animal, frozen on dry ice and then stored at -80°C. RNA from each subregion of individual animals was processed and hybridized to separate arrays.

RNA Quality Control, cRNA Labeling, and Microarray Hybridization: RNA samples were sent to the The Johns Hopkins Microarray core facility for quality assessment, cRNA labeling, and hybridization to Affymetrix RAE230A microarrays. RNA quality was assessed using Agilent Bioanalyzer. Ribosomal RNA ratio (28S:18S around 2.0) as well as RNA integrity number (RIN > 7.0) were used to verify RNA quality. All samples met quality standards for microarray analysis.

cRNA labeling from RNA samples was performed following Affymetrix specifications. Briefly, 5 μg of total RNA was used to synthesize first strand cDNA using oligonucleotide probes with 24 oligo-dT plus T7 promoter as primer (Proligo LLC), and

the SuperScript Choice System (Invitrogen). Following the double stranded cDNA synthesis, the product was purified by phenol-chloroform extraction, and biotinilated anti-sense cRNA was generated through *in vitro* transcription using the BioArray RNA High Yield Transcript Labelling kit (ENZO Life Sciences Inc). 15 µg of the biotinilated cRNA was fragmented at 94°C for 35 min (100mM Trix-acetate, pH 8.2, 500mM KOAc, 150mM MgOAC), and 10µg of total fragmented cRNA was hybridized to the Affymetrix GeneChip arrays for 16hr at 45°C with constant rotation (60 rpm). Affymetrix Fluidics Station 450 was then used to wash and stain the Chips, removing the non-hybridized target and incubating with a streptavidin-phycoerythrin conjugate to stain the biotinilated cRNA. The staining was then amplified using goat IgG as blocking reagent and biotinilated anti-streptavidin antibody (goat), followed by a second staining step with a streptavidin-phycoerythrin conjugate. Fluorescence was detected using the Affymetrix G3000 GeneArray Scanner and image analysis of each GeneChip was done through the GeneChip Operating System 1.1.1 (GCOS) software from Affymetrix, using the standard default settings.

Microarray Data Quality Control and Normalization: All quality control, normalization, differential expression, and exploratory analysis of microarray data were performed using the open-source R statistical language (http://www.r-project.org/). Raw CEL files from individual hybridizations were imported using the "affy" package in the Bioconductor (Irizarry et al., 2003)(http://www.bioconductor.org/) collection of R packages. Quality of microarray data was assessed on many levels: RNA degradation plots were created to examine signal intensities of probes on the microarray as a function of their 3' - 5'

position in the transcript being interrogated. This serves primarily as a post-experiment inspection of RNA quality/integrity. Raw, log2, and normalized (see below) intensities and ratios to mean intensities were inspected using boxplots, density estimates, and scatter plots in order to check for intensity-based artifacts. Chip pseudo images were created from both intensity and ratio data in order to detect any spatial hybridization artifacts. Several dimension reducing algorithms, including principal component analysis (PCA), multidimensional scaling (MDS), and clustering were used to assess variance globally across all expression measures and to identify outlier microarrays. Based on these data, 5 arrays were excluded from further analysis (1 AU in each of CA1, CA3 and dentate gyrus as well as 1 Y and 1 AI dentate gyrus array) resulting in 6 AU, 8AI and 9Y arrays for CA1 and CA3 and 6 AU, 7 AI and 8Y arrays for dentate gyrus. The "gcrma" package in Bioconductor was used to normalize microarray data following quality control procedures. This involves background correction, quantile normalization, and probeset summarization.

Differential Expression of Individual Genes: Significance Analysis in Microarrays d-statistics (Tusher et al., 2001) were used to assess differential expression across groups of animals. This entails a moderated T-statistic which borrows variance information across genes in order to increase statistical power and to avoid the tendency to find low variance expression changes significant. In addition, an empirically determined low intensity limit was used. This limit was determined by inspecting differential expression statistics across the range of intensity measures. As is common in Affymetrix data normalized with GCRMA, there was a clear level below which differential expression statistics showed

markedly different behavior with regards to variance and bias yielding a bimodal distribution of intensities in the $\log_2$ scale. In all three datasets, this distribution had a clear minimum between the two modes where we placed our low-intensity cut-off. In this case it was at a value of 5 in the $\log_2$ scale for all datasets. Expression values below this limit were omitted from the analysis of differential expression of individual genes. Because GCRMA includes quantile normalization, each of the arrays will have a near identical distribution of intensities and hence this cut-off is appropriate for all arrays. In order to assess differential expression associated with specific phenotypes subjects were grouped together for specific comparison: age phenotype (Y vs AU+AI), impaired phenotype (AI v AU+Y) and cognition within aging (AI v AU). Numbers of probesets with SAM p-value < 0.05 are listed in Table S2. To control for false positives introduced by large numbers of comparisons, false discovery rate (FDR) analysis was used to create gene lists containing a precisely estimated proportion of false hits. This is achieved by comparing the observed differential expression statistics to those expected by chance. Those expected by chance are estimated by permuting the group labels of the data many times and recalculating differential expression statistics.

Multidimensional Scaling analysis (MDS): Using all 15,923 gene expression measures generated from each microarray, the pair-wise correlation (r) between all possible sample pairs was calculated. An MDS algorithm was used to represent all pair-wise distances (defined to be 1-r) such that each sample was visualized as a single point in 2D space.

In situ probe generation: BIP/GRP78/HSPA5, and calreticulin riboprobe template constructs were generated by PCR amplification from rodent hippocampal cDNA. Two sets of primers were used for each gene such that appropriate overhangs were generated after dissociation and re-annealing of the amplified products (Zeng, 1998); BIP primers: Left A: 5'agcttcaggatgcagacattgaagac, Left B: 5'tcaggatgcagacattgaagac, Right A: 5'catccaaggtgaacacacacc, Right B: 5'aattcatccaaggtgaacacacacc; Calreticulin primers: Left A: 5'agcttgtactgggcttagacctctgg, Left B: 5'tgtactgggcttagacctctgg, Right A: 5'cgcctctacagctcatccttg, Right B: 5'aattcgcctctacagctcatccttg. The resulting templates were cloned into the EcoRI and HindIII sites of pGEM7zf+ (Promega). Lpl , Gabra 5, Tcp1 probes were generated by PCR amplification from rodent hippocampal cDNA (Lpl primers – left: 5'cctgactccaatgtcattgtag , right 5'acttcaccagctggtccacatc; Gabra5 primers – left: 5'gaatctgtcccagctaggac, right: 5'ctctcagaagtcttctcctc ; TCP1 primers -left: 5'ggagaggatttgtgacgatg, right: 5'gctcttaacttggcaaccag) followed by a second round of amplification with primers containing Sp6 and T7 polymerase binding sites. ^{35}S-UTP labeled riboprobes were generated using the Maxiscript kit (Ambion) according to manufacturer's directions. The probe was then phenol/choloroform extracted, ethanol precipitated at -80°C, and resuspended in RNase-free water.

In situ hybridization: Aged and young rats were behaviorally characterized using the same protocol as for the microarray. For LPL and GABRA5 resulting Ns were 5Y, 5AU and 6AI and for Tcp1, BiP and Calr, Ns were 5Y, 6AU and 6AI. The rats were anesthetized with isoflurane and transcardially perfused with 0.1 M phosphate buffer saline at room temperature followed by ice-cold 4% paraformaldehyde (PFA) in 0.1 M

phosphate buffer (PB). Brains were removed and post-fixed in 4% PFA at 4°C for an additional 24 hr, and then transferred to 20% sucrose in 4% PFA at 4°C for another 24 hr. The brains were then stored at -80°C until sectioning. Blocks of brains containing the hippocampus were sectioned at 30 mm thickness, and stored free-floating in 4% PFA for at least 3 weeks. All sections for each gene analysis were hybridized simultaneously using a single probe preparation. Prior to hybridization, brain sections were washed twice in 0.75% glycine in 0.1 M PB, once in 0.1 M PB, and then incubated in Proteinase K (1 mg/ml) for 30 min at 37°C. The Proteinase K reaction was stopped by a 10 minute incubation in acetic anhydride solution (1.3%Triethanolamine, 0.25% Acetic anhydride, 0.04 M Acetic acid) followed by 2 washes in 2X SSC (20X = 3 M sodium chloride and 0.3 M sodium citrate). Sections were hybridized overnight at 60°C in hybridization buffer (20% formamide, 0.4X Denhardt's solution, 4% dextran sulfate and 1.6X SSC) supplemented with 0.25 mg/ml tRNA, 0.33 mg/ml sheared salmon sperm DNA, 100 mM Dithiothreitol (DTT) and 1 x 10^7 cpm/ml ^{35}S-UTP labeled probe. After hybridization, sections were washed at 60°C in 4X SSC/0.01 M DTT twice and once in 2X SSC/ 50% formamide. They were then washed twice in RNase buffer (5 mM Tris at pH 8.0, 0.5 M sodium chloride, and 1 mM EDTA) and incubated with RNase (20 ug/ml) at 37°C for 30 minutes. Sections were washed twice at room temperature in 2X SSC, and twice each in 0.5X SSC and 0.1X SSC at 60°C before mounting onto slides. Slides were dried overnight and exposed to a phosphoimager screen, and analyzed with ImageQuant (Amersham Biosciences). Processing and analyzing of the brain sections were done blind to experimental conditions. For each animal 3-5 matched brain sections were analyzed including the left and the right hippocampi and restricted to the dorsal hippocampus.

Either whole hippocampus, complete CA3 or complete CA1 were outlined by hand within the image quant program. The anterior-posterior level of brain sections analyzed were approximately 2.12 to 4.16 mm posterior to bregma (Paxinos & Watson, 1986). Radioactive standards exposed at the same time as the sections ensured that section intensity was within the linear range. Preliminary analyses showed little differences in mRNA expression levels across the anterior-posterior levels of the dorsal hippocampus; hence, we averaged the expression intensity of all sections for each rat. Because of occasional variability in hybridization, outliers were removed based on the formula *median ± 2(Q3-Q1)*. Analysis of variance was used to determine significant differences between groups.

Immunohistochemistry: Aged and young rats were behaviorally characterized using the same protocol as for the microarray. Total N of 23 consisted of 8Y, 8AU, and 7AI. The rats were anesthetized with isoflurane and transcardially perfused with 0.1 M phosphate buffer saline (PBS) at room temperature followed by ice-cold 4% paraformaldehyde (PFA) in 0.1 M phosphate buffer (PB). Brains were removed and post-fixed in 4% PFA at 4°C for an additional 24 hr, and then transferred to 20% sucrose in 4% PFA at 4°C for another 24 hr. The brains were then stored at -80°C until sectioning. Blocks of brains containing the hippocampus were sectioned at 40 μm thickness, and stored free-floating in 4% PFA for at least 3 weeks. Histological sections were labeled with a commercially available Neuromab, monoclonal antibody against Kv4.2 (1:500); Antibodies Inc., Davis, CA). Characteristic staining and antibody specificity has been previously demonstrated for the Kv4.2 antibody utilized (Varga et al., 2000). All tissue from each animal group

was processed concurrently (8Y, 8AU, 7AI). Free-floating sections were washed in 0.1M PBS at room temperature (5x10 min), incubated in 0.3% H_2O_2 in 0.1M PBS (30 min), and then washed in 0.1M PBS (3x10 min). Tissue was then blocked in PBST (0.1 M PBS and 0.3% triton) and 6% normal goat serum (NGS) for 1 hr at room temperature and subsequently washed in 0.1M PBS (3X5 min). Tissue was then incubated for 72 hrs at 4°C with Kv4.2 antibody diluted in PBST (1:500 antibody dilution, 0.1 M PBS and 0.15% triton) with 3% NGS. Tissue sections were removed from antibody dilution, rinsed in 0.1M PBS (4x5 min), and incubated for 1 hr at room temperature with goat anti-mouse secondary antibody (1:250 antibody dilution; Vector Laboratories.) in PBST (0.1 M PBS and 0.15% triton) with 3% NGS. Sections were washed in 0.1M PBS (3x10 min), incubated in ABC reagent (Vector Laboratories) in 0.1M PBS for 1 hr, and then rinsed in 0.1M PBS (3x10 min). Tissue was then color reacted with DAB (Vector Laboratories), given a final rise in 0.1M PBS (3x10 min), and then mounted on slides and left to dry for 24 hrs at room temperature and then oven dried for 24 hrs. Slides were coverslipped using a xylene-based medium and stored until analysis. Analyses were restricted to the dorsal hippocampus. The anterior-posterior level of brain sections analyzed was approximately 2.80 to 3.30 mm posterior to bregma (Paxinos & Watson, 1986). For each rat, hippocampi were analyzed across 3-4 matched sections, including the left and right hippocampi. Protein expression levels were quantified for each animal with the open source program ImageJ. The subregion of interest was outlined by a researcher who was blind to group conditions. Furthermore, a pixel by pixel analysis of protein expression for each animal was taken from a 150µm section in CA3b in a soma-dendritic pattern to observe levels of Kv4.2 expression along the dendritic trajectory from soma to stratum

lacunosum-moleculare. Four points of protein expression along this path, corresponding to important anatomical markers for the pyramidal cell body, stratum lucidum-stratum radiatum border, stratum radiatum, and stratum lacunosum-moleculare, were compared between groups. Tissue sections were averaged to obtain a single expression score for each animal and data was statistically analyzed with a one-way ANOVA (regional analysis) and two-way repeated measures ANOVA (CA3b dendritic analysis). Post-hoc analyses were conducted using a set of predetermined Scheffe's contrasts, corrected for multiple comparisons.

Supplemental References:

Gallagher M, Colantuoni C, Eichenbaum H, Haberman RP, Rapp PR, Tanila H, Wilson IA (2006) Individual differences in neurocognitive aging of the medial temporal lobe. AGE: Journal of the American Aging Association 28:221-223.

Irizarry RA, Hobbs B, Collin F, Beazer-Barclay YD, Antonellis KJ, Scherf U, Speed TP (2003) Exploration, normalization, and summaries of high density oligonucleotide array probe level data. Biostatistics 4:249-264.

Tusher VG, Tibshirani R, Chu G (2001) Significance analysis of microarrays applied to the ionizing radiation response. Proc Natl Acad Sci U S A 98:5116-5121.

Varga AW, Anderson AE, Adams JP, Vogel H, Sweatt JD (2000) Input-specific immunolocalization of differentially phosphorylated Kv4.2 in the mouse brain. Learn Mem 7:321-332.

Zeng G (1998) Sticky-end PCR: new method for subcloning. Biotechniques 25:206-208.

Supplemental Figure legends:

Figure S1: Hidden platform watermaze training data for all rats included in the microarray analysis. Performance on the first training trial does not differ between aged and young rats, as indicated by cumulative search error, but during training aged rats exhibit poorer learning. Repeated measures anova confirms highly significant group and trial differences (all $p<0.0001$). Error bars indicate standard error of the mean.

Figure S2: **A.** Global data analysis by multidimensional scaling (MDS). Each point within the graph represents a single array colored by cognitive group (Y, black; AU, red; AI, blue) and distance between points is an indication of relative similarity of mRNA profiles. As with PCA, AU subjects form a distinct group, separated along both dimensions, from both young and aged impaired in CA3. In CA1 AU arrays fall in between AI and Y. The middle panel (CA3) has been reprinted with permission from Gallagher et al (2006). **B.** Graphical visualization of SAM d-statistic distributions illustrates significant CA3 expression changes associated with aging. The density of observed d-statistic distributions (black lines) were plotted for the chronological age comparison consisting of all aged subjects compared to Y (AI+AU v Y) for each subregion. The distribution expected by chance (green line) was used to determine the

false detection rate (FDR; see methods for details). Dotted vertical lines to the left and right demarcate the point beyond which the false detection rate is 5%. Differentially expressed probe sets exceeding this FDR are represented by the shaded space between the green and black lines to the outside of the dotted lines and the numbers are noted on each graph. Numbers on the x-axis to the right (positive d-stat) indicate increased expression and numbers to the left (negative d-stat) indicate decreased expression in all aged subjects.

Figure S3. In situ hybridization analysis of Tcp1 and Hspa5/BiP. Images of representative matched sections hybridized to radiolabeled Tcp1 (Left column) or Hspa5/BiP (right column) probe and exposed to film. Images were pseudocolored to better define expression differences. Intensity scale is depicted below the images.

Figure S4. Immunohistochemical analysis of Kv4.2 protein. Images of representative young, aged unimpaired and aged impaired hippocampal sections stained with antibody to Kv4.2. Box delineates the area analyzed in Figure 6C.

Table S1. Functional groups analysis for chronological age comparison (AI+AU v Y) for each subregion: GO, Kegg, Pfam and protein binding groups with p<0.001.

Group ID[a]	Group name	Direction[b]	WRSp[c]
	CA3		
GO:0006414	translational elongation	Up	0.00
Kegg03010	Ribosome	Up	0.00
GO:0003735	structural constituent of ribosome	Up	0.00
GO:0022627	cytosolic small ribosomal subunit	Up	6.88E-14
GO:0005840	ribosome	Up	7.09E-13
GO:0006412	translation	Up	1.19E-11
GO:0005764	lysosome	Up	1.44E-08
GO:0005576	extracellular region	Up	1.17E-06
Kegg04610	Complement and coagulation cascades	Up	7.18E-06
GO:0005245	voltage-gated calcium channel activity	Down	1.54E-05
PB:1508	CTSB	Up	2.57E-05
PF00118	TCP-1/cpn60 chaperonin family	Down	3.01E-05
PB:7203	CCT3	Down	3.24E-05
PF00112	Papain family cysteine protease	Up	3.40E-05
PB:9051	PSTPIP1	Up	3.83E-05
GO:0005615	extracellular space	Up	4.18E-05
GO:0051246	regulation of protein metabolic process	Down	4.39E-05
Kegg04060	Cytokine-cytokine receptor interaction	Up	4.87E-05
PF00096	Zinc finger, C2H2 type	Up	6.79E-05
GO:0005891	voltage-gated calcium channel complex	Down	8.38E-05
GO:0004364	glutathione transferase activity	Up	0.00010
GO:0019843	rRNA binding	Up	0.00013
PB:5347	PLK1	Down	0.00015
PB:4113	MAGEB2	Up	0.00016

GO:0005643	nuclear pore	Down	0.00016
PB:7555	CNBP	Up	0.00018
Kegg00480	Glutathione metabolism	Up	0.00018
Kegg03050	Proteasome	Down	0.00019
PF01023	S-100/ICaBP type calcium binding domain	Up	0.00020
GO:0003674	molecular_function	Up	0.00021
GO:0006355	regulation of transcription, DNA-dependent	Up	0.00024
PF00244	14-3-3 protein	Down	0.00024
PF00179	Ubiquitin-conjugating enzyme	Down	0.00025
GO:0004714	transmembrane receptor protein tyrosine kinase activity	Up	0.00028
GO:0030117	membrane coat	Down	0.00030
GO:0000028	ribosomal small subunit assembly and maintenance	Up	0.00030
GO:0007268	synaptic transmission	Down	0.00031
GO:0008150	biological_process	Up	0.00035
PB:712	C1QA	Up	0.00036
GO:0006606	protein import into nucleus	Down	0.00038
GO:0007269	neurotransmitter secretion	Down	0.00043
GO:0019787	small conjugating protein ligase activity	Down	0.00047
PB:9610	RIN1	Down	0.00048
GO:0005737	cytoplasm	Down	0.00050
PB:7187	TRAF3	Down	0.00051
PB:10808	HSPH1	Down	0.00056
PB:22933	SIRT2	Down	0.00059
PF00178	Ets-domain	Up	0.00064
PB:2	A2M	Up	0.00064
GO:0046961	hydrogen ion transporting ATPase activity, rotational mechanism	Down	0.00069
PF08246	Cathepsin propeptide inhibitor domain (I29)	Up	0.00072
PB:5923	RASGRF1	Down	0.00075

PB:4140	MARK3	Down	0.00079
Kegg00980	Metabolism of xenobiotics by cytochrome P450	Up	0.00080
GO:0006817	phosphate transport	Up	0.00081
PF01556	DnaJ C terminal region	Down	0.00081
PF00498	FHA domain	Up	0.00086
PB:5894	RAF1	Down	0.00086
Kegg00190	Oxidative phosphorylation	Down	0.00091
GO:0043169	cation binding	Up	0.00093
GO:0043687	post-translational protein modification	Down	0.00096
GO:0019904	protein domain specific binding	Down	0.00096
PB:4686	NCBP1	Down	0.00098
GO:0005164	tumor necrosis factor receptor binding	Up	0.00098
	CA1		
GO:0006414	translational elongation	Up	0
Kegg03010	Ribosome	Up	0
GO:0003735	structural constituent of ribosome	Up	0
GO:0005840	ribosome	Up	4.44E-16
GO:0022627	cytosolic small ribosomal subunit	Up	2.15E-12
GO:0006412	translation	Up	4.48E-12
GO:0005764	lysosome	Up	3.36E-11
GO:0005739	mitochondrion	Up	1.08E-09
GO:0055114	oxidation reduction	Up	2.18E-08
GO:0016491	oxidoreductase activity	Up	3.41E-07
GO:0006979	response to oxidative stress	Up	2.17E-06
GO:0006629	lipid metabolic process	Up	4.16E-06
GO:0006749	glutathione metabolic process	Up	4.40E-06
Kegg00071	Fatty acid metabolism	Up	7.50E-06
Kegg00480	Glutathione metabolism	Up	8.96E-06
Kegg04360	Axon guidance	Down	9.51E-06

Kegg00980	Metabolism of xenobiotics by cytochrome P450	Up	9.77E-06
Kegg04610	Complement and coagulation cascades	Up	9.96E-06
Kegg01032	Glycan structures - degradation	Up	1.87E-05
GO:0005829	cytosol	Up	1.94E-05
GO:0008152	metabolic process	Up	2.67E-05
PB:8648	NCOA1	Down	3.06E-05
GO:0004364	glutathione transferase activity	Up	5.66E-05
Kegg00280	Valine, leucine and isoleucine degradation	Up	8.56E-05
GO:0006817	phosphate transport	Up	0.00010
GO:0005164	tumor necrosis factor receptor binding	Up	0.00013
GO:0043169	cation binding	Up	0.00014
Kegg00982	Drug metabolism - cytochrome P450	Up	0.00014
Kegg00511	N-Glycan degradation	Up	0.00014
GO:0005884	actin filament	Up	0.00016
GO:0005975	carbohydrate metabolic process	Up	0.00018
GO:0042612	MHC class I protein complex	Up	0.00021
GO:0003674	molecular_function	Up	0.00023
PF00129	Class I Histocompatibility antigen, domains alpha 1 and 2	Up	0.00025
GO:0043295	glutathione binding	Up	0.00026
PF00229	TNF(Tumour Necrosis Factor) family	Up	0.00029
GO:0007040	lysosome organization and biogenesis	Up	0.00029
Kegg04540	Gap junction	Down	0.00032
Kegg00640	Propanoate metabolism	Up	0.00032
PB:7203	CCT3	Down	0.00035
PF07654	Immunoglobulin C1-set domain	Up	0.00041
Kegg04310	Wnt signaling pathway	Down	0.00043
GO:0006955	immune response	Up	0.00043
PF00191	Annexin	Up	0.00045
PF00112	Papain family cysteine protease	Up	0.00048

PF06623	MHC_I C-terminus	Up	0.00051
GO:0006508	proteolysis	Up	0.00051
PF00788	Ras association (RalGDS/AF-6) domain	Up	0.00053
PB:23523	CABIN1	Down	0.00053
GO:0006958	complement activation, classical pathway	Up	0.00062
PB:5599	MAPK8	Up	0.00073
GO:0016272	prefoldin complex	Up	0.00075
GO:0003702	RNA polymerase II transcription factor activity	Up	0.00077
PF03179	Vacuolar (H+)-ATPase G subunit	Up	0.00080
PB:4113	MAGEB2	Up	0.00082
GO:0005643	nuclear pore	Down	0.00083
GO:0009055	electron carrier activity	Up	0.00088
GO:0002474	antigen processing and presentation of peptide antigen via MHC class I	Up	0.00090
PF00118	TCP-1/cpn60 chaperonin family	Down	0.00091
GO:0008150	Biological process	Up	0.00098

Dentate Gyrus

PF07654	Immunoglobulin C1-set domain	Up	1.39E-05
PB:1855	DVL1	Down	2.58E-05
GO:0042612	MHC class I protein complex	Up	2.96E-05
PF00129	Class I Histocompatibility antigen, domains alpha 1 and 2	Up	3.41E-05
GO:0006955	immune response	Up	3.66E-05
GO:0005164	tumor necrosis factor receptor binding	Up	4.09E-05
GO:0002474	antigen processing and presentation of peptide antigen via MHC class I	Up	4.65E-05
PB:5757	PTMA	Down	5.16E-05
GO:0005743	mitochondrial inner membrane	Down	5.45E-05
PF00229	TNF(Tumour Necrosis Factor) family	Up	5.55E-05
PB:338	APOB	Down	8.28E-05
GO:0048469	cell maturation	Down	9.32E-05

PB:7203	CCT3	Down	9.73E-05
PF00505	HMG (high mobility group) box	Down	0.00010
GO:0005764	lysosome	Up	0.00010
PF06623	MHC_I C-terminus	Up	0.00012
GO:0019882	antigen processing and presentation	Up	0.00015
PF00754	F5/8 type C domain	Up	0.00015
GO:0046873	metal ion transmembrane transporter activity	Up	0.00015
GO:0005884	actin filament	Up	0.00016
GO:0005576	extracellular region	Up	0.00018
PF00112	Papain family cysteine protease	Up	0.00020
GO:0006817	phosphate transport	Up	0.00030
PF00118	TCP-1/cpn60 chaperonin family	Down	0.00033
GO:0008378	galactosyltransferase activity	Up	0.00038
Kegg01032	Glycan structures - degradation	Up	0.00039
GO:0019885	antigen processing and presentation of endogenous peptide antigen via MHC class I	Up	0.00041
GO:0047915	ganglioside galactosyltransferase activity	Up	0.00041
PF03344	Daxx Family	Up	0.00041
PF03849	Transcription factor Tfb2	Up	0.00041
PF05083	LST-1 protein	Up	0.00041
PF08149	BING4CT (NUC141) domain	Up	0.00041
GO:0016272	prefoldin complex	Up	0.00043
GO:0001891	phagocytic cup	Up	0.00043
GO:0050681	androgen receptor binding	Up	0.00054
PF01556	DnaJ C terminal region	Down	0.00061
PF01410	Fibrillar collagen C-terminal domain	Up	0.00065
Kegg04530	Tight junction	Down	0.00065
GO:0008013	beta-catenin binding	Down	0.00071
PF00157	Pou domain - N-terminal to homeobox domain	Up	0.00078
GO:0001764	neuron migration	Down	0.00080

PF02535	ZIP Zinc transporter	Up	0.00085
PF01391	Collagen triple helix repeat (20 copies)	Up	0.00087
GO:0004519	endonuclease activity	Up	0.00089
GO:0042613	MHC class II protein complex	Up	0.00092
PF00993	Class II histocompatibility antigen, alpha domain	Up	0.00092
PB:1499	CTNNB1	Down	0.00093
PB:29993	PACSIN1	Up	0.00096
PF03179	Vacuolar (H+)-ATPase G subunit	Up	0.00099

[a]GO, gene ontology; KEGG, Kyoto Encyclopedia of Genes and Genomes; PF, PFAM protein sequence motifs; PB, protein binding (NCBI protein-protein interactions based on human interactions)

[b]Indicates direction of change in aged subjects relative to young.

[c]Uncorrected Wilcox rank sum p-value.

Table S2. Numbers of probesets with p-value <0.05 for SAM analysis (left columns) or MAS5.0 analysis (right columns) for each comparison within each subregion.

Group Comparison	gcRMA (SAMp<0.05)			MAS5.0 (Ttestp<0.05)		
	CA1	CA3	DG	CA1	CA3	DG
AI+AU v Y	2058	3392	1865	1512	3217	1955
AI v AU+Y	1712	2924	1699	1325	3171	1739
AI v AU	1265	1827	2045	826	2018	1912

Table S3. Functional groups analysis for age impaired comparison (AI v AU+Y) for each subregion: GO, Kegg, Pfam and protein binding groups with $p<0.001$.

Group ID[a]	Group name	Direction[b]	WRSp[c]
	CA3		
GO:0006414	translational elongation	Up	0.00
Kegg03010	Ribosome	Up	0.00
GO:0022627	cytosolic small ribosomal subunit	Up	1.83E-10
GO:0003735	structural constituent of ribosome	Up	4.03E-10
GO:0005840	ribosome	Up	1.19E-08
GO:0005764	lysosome	Up	1.14E-06
GO:0005576	extracellular region	Up	1.55E-06
GO:0006412	translation	Up	1.80E-06
Kegg04610	Complement and coagulation cascades	Up	1.42E-05
GO:0005615	extracellular space	Up	2.52E-05
GO:0006817	phosphate transport	Up	5.09E-05
Kegg04060	Cytokine-cytokine receptor interaction	Up	6.49E-05
GO:0051246	regulation of protein metabolic process	Down	8.63E-05
GO:0019843	rRNA binding	Up	0.00010
PF00244	14-3-3 protein	Down	0.00014
GO:0005245	voltage-gated calcium channel activity	Down	0.00016
Kegg00190	Oxidative phosphorylation	Down	0.00018
PF00118	TCP-1/cpn60 chaperonin family	Down	0.00022
GO:0046961	hydrogen ion transporting ATPase activity, rotational mechanism	Down	0.00027
PB:7203	CCT3	Down	0.00028
PF00112	Papain family cysteine protease	Up	0.00029
GO:0009611	response to wounding	Up	0.00032
GO:0006955	immune response	Up	0.00032

PF00386	C1q domain	Up	0.00033
PB:1508	CTSB	Up	0.00042
PB:3952	LEP	Up	0.00045
GO:0015992	proton transport	Down	0.00047
GO:0016469	proton-transporting two-sector ATPase complex	Down	0.00048
GO:0019882	antigen processing and presentation	Up	0.00054
PB:7187	TRAF3	Down	0.00065
PB:673	BRAF	Down	0.00066
Kegg00980	Metabolism of xenobiotics by cytochrome P450	Up	0.00076
GO:0004364	glutathione transferase activity	Up	0.00077
PF01391	Collagen triple helix repeat (20 copies)	Up	0.00081
Kegg00982	Drug metabolism - cytochrome P450	Up	0.00085
PB:5923	RASGRF1	Down	0.00092
GO:0046933	hydrogen ion transporting ATP synthase activity, rotational mechanism	Down	0.00094
PF01023	S-100/ICaBP type calcium binding domain	Up	0.00094
PF01556	DnaJ C terminal region	Down	0.00099

CA1

GO:0006414	translational elongation	Up	0.00
Kegg03010	Ribosome	Up	2.22E-15
GO:0005764	lysosome	Up	3.48E-12
GO:0055114	oxidation reduction	Up	2.94E-11
GO:0016491	oxidoreductase activity	Up	1.67E-10
GO:0003735	structural constituent of ribosome	Up	2.01E-10
GO:0005840	ribosome	Up	8.84E-10
GO:0005829	cytosol	Up	3.09E-09
GO:0005739	mitochondrion	Up	6.21E-09
GO:0022627	cytosolic small ribosomal subunit	Up	1.07E-08
GO:0006412	translation	Up	1.40E-08
GO:0008152	metabolic process	Up	1.89E-08

GO:0006629	lipid metabolic process	Up	6.98E-08
Kegg00480	Glutathione metabolism	Up	5.86E-07
GO:0006817	phosphate transport	Up	6.47E-07
GO:0005625	soluble fraction	Up	7.51E-07
Kegg00071	Fatty acid metabolism	Up	1.56E-06
GO:0006749	glutathione metabolic process	Up	1.64E-06
Kegg04060	Cytokine-cytokine receptor interaction	Up	6.99E-06
Kegg00982	Drug metabolism - cytochrome P450	Up	8.74E-06
Kegg00980	Metabolism of xenobiotics by cytochrome P450	Up	1.61E-05
Kegg00010	Glycolysis / Gluconeogenesis	Up	1.69E-05
GO:0006979	response to oxidative stress	Up	2.32E-05
GO:0006955	immune response	Up	3.04E-05
GO:0005884	actin filament	Up	6.78E-05
PB:8648	NCOA1	Down	6.89E-05
PF00229	TNF(Tumour Necrosis Factor) family	Up	7.03E-05
Kegg00590	Arachidonic acid metabolism	Up	7.08E-05
GO:0005164	tumor necrosis factor receptor binding	Up	7.97E-05
Kegg04610	Complement and coagulation cascades	Up	8.82E-05
GO:0006096	glycolysis	Up	9.25E-05
GO:0006635	fatty acid beta-oxidation	Up	0.00013
GO:0006508	proteolysis	Up	0.00013
GO:0016829	lyase activity	Up	0.00015
GO:0005759	mitochondrial matrix	Up	0.00017
PF01410	Fibrillar collagen C-terminal domain	Up	0.00018
Kegg00280	Valine, leucine and isoleucine degradation	Up	0.00018
PB:57180	ACTR3B	Down	0.00019
Kegg01032	Glycan structures - degradation	Up	0.00020
Kegg00251	Glutamate metabolism	Up	0.00024
PF01391	Collagen triple helix repeat (20 copies)	Up	0.00025
PF07654	Immunoglobulin C1-set domain	Up	0.00025

GO:0042612	MHC class I protein complex	Up	0.00026
GO:0016272	prefoldin complex	Up	0.00027
PB:821	CANX	Up	0.00033
GO:0043295	glutathione binding	Up	0.00034
GO:0001891	phagocytic cup	Up	0.00039
PF03179	Vacuolar (H+)-ATPase G subunit	Up	0.00039
GO:0004364	glutathione transferase activity	Up	0.00040
GO:0000902	cell morphogenesis	Up	0.00044
PF01920	Prefoldin subunit	Up	0.00046
PB:5599	MAPK8	Up	0.00047
GO:0051287	NAD binding	Up	0.00047
PB:476	ATP1A1	Up	0.00051
GO:0042744	hydrogen peroxide catabolic process	Up	0.00051
GO:0005615	extracellular space	Up	0.00052
Kegg00640	Propanoate metabolism	Up	0.00054
PF00129	Class I Histocompatibility antigen, domains alpha 1 and 2	Up	0.00055
PB:10097	ACTR2	Down	0.00059
PB:10109	ARPC2	Down	0.00059
PB:10094	ARPC3	Down	0.00059
PB:10093	ARPC4	Down	0.00059
GO:0000287	magnesium ion binding	Up	0.00062
PB:7067	THRA	Down	0.00064
Kegg00310	Lysine degradation	Up	0.00065
Kegg00511	N-Glycan degradation	Up	0.00066
GO:0014070	response to organic cyclic substance	Up	0.00067
PB:6844	VAMP2	Up	0.00068
GO:0019885	antigen processing and presentation of endogenous peptide antigen via MHC class I	Up	0.00073
GO:0047915	ganglioside galactosyltransferase activity	Up	0.00073

PF03344	Daxx Family	Up	0.00073
PF03849	Transcription factor Tfb2	Up	0.00073
PF05083	LST-1 protein	Up	0.00073
PF08149	BING4CT (NUC141) domain	Up	0.00073
GO:0008144	drug binding	Up	0.00080
Kegg00120	Bile acid biosynthesis	Up	0.00082
GO:0009055	electron carrier activity	Up	0.00083
PB:5578	PRKCA	Up	0.00084
PB:7068	THRB	Down	0.00085
PF00169	PH domain	Up	0.00086
PB:6810	STX4	Up	0.00086
PF02373	JmjC domain	Down	0.00089
PB:3675	ITGA3	Up	0.00090
PF00884	Sulfatase	Up	0.00099

Dentate Gyrus

GO:0005164	tumor necrosis factor receptor binding	Up	2.33E-06
GO:0016272	prefoldin complex	Up	2.50E-06
PF00229	TNF(Tumour Necrosis Factor) family	Up	4.58E-06
GO:0005764	lysosome	Up	7.64E-06
GO:0005884	actin filament	Up	2.50E-05
PF00498	FHA domain	Up	2.78E-05
GO:0019885	antigen processing and presentation of endogenous peptide antigen via MHC class I	Up	4.16E-05
GO:0047915	ganglioside galactosyltransferase activity	Up	4.16E-05
PF03344	Daxx Family	Up	4.16E-05
PF03849	Transcription factor Tfb2	Up	4.16E-05
PF05083	LST-1 protein	Up	4.16E-05
PF08149	BING4CT (NUC141) domain	Up	4.16E-05
PF03179	Vacuolar (H+)-ATPase G subunit	Up	4.66E-05
GO:0050681	androgen receptor binding	Up	5.49E-05

PF00788	Ras association (RalGDS/AF-6) domain	Up	5.78E-05
GO:0001891	phagocytic cup	Up	7.40E-05
PB:6643	SNX2	Up	8.14E-05
PF00618	Guanine nucleotide exchange factor for Ras-like GTPases; N-terminal motif	Up	0.00010
GO:0042613	MHC class II protein complex	Up	0.00011
PF00993	Class II histocompatibility antigen, alpha domain	Up	0.00011
GO:0000281	cytokinesis after mitosis	Up	0.00012
GO:0042612	MHC class I protein complex	Up	0.00013
GO:0002474	antigen processing and presentation of peptide antigen via MHC class I	Up	0.00015
PB:7203	CCT3	Down	0.00016
PF01920	Prefoldin subunit	Up	0.00016
GO:0016787	hydrolase activity	Up	0.00022
GO:0042803	protein homodimerization activity	Up	0.00022
PF00112	Papain family cysteine protease	Up	0.00024
GO:0046873	metal ion transmembrane transporter activity	Up	0.00028
PB:54453	RIN2	Up	0.00028
Kegg01032	Glycan structures - degradation	Up	0.00029
GO:0005625	soluble fraction	Up	0.00029
PF07654	Immunoglobulin C1-set domain	Up	0.00033
GO:0003702	RNA polymerase II transcription factor activity	Up	0.00039
PB:10567	RABAC1	Up	0.00040
PB:580	BARD1	Up	0.00040
GO:0051017	actin filament bundle formation	Up	0.00042
PF06623	MHC_I C-terminus	Up	0.00043
PF02535	ZIP Zinc transporter	Up	0.00043
Kegg00511	N-Glycan degradation	Up	0.00044
GO:0000792	heterochromatin	Up	0.00046
GO:0008378	galactosyltransferase activity	Up	0.00047

PF00616	GTPase-activator protein for Ras-like GTPase	Up	0.00061
GO:0007169	transmembrane receptor protein tyrosine kinase signaling pathway	Up	0.00061
PF01762	Galactosyltransferase	Up	0.00064
PB:112755	STX1B	Up	0.00074
Kegg01030	Glycan structures - biosynthesis 1	Down	0.00074
GO:0003676	Nucleic acid binding	Up	0.00083
Kegg05217	Basal cell carcinoma	Down	0.00085
PB:3191	HNRNPL	Up	0.00085
GO:0030154	cell differentiation	Up	0.00088
PB:3953	LEPR	Up	0.00091
PF00129	Class I Histocompatibility antigen, domains alpha 1 and 2	Up	0.00097

[a]GO, gene ontology; KEGG, Kyoto Encyclopedia of Genes and Genomes; PF, PFAM protein sequence motifs ; PB, protein binding (NCBI protein-protein interactions)

[b]Indicates direction of change in aged impaired subjects relative to the combined group of young and aged unimpaired.

[c]Uncorrected Wilcox rank sum p-value.

Haberman et al, Figure S1

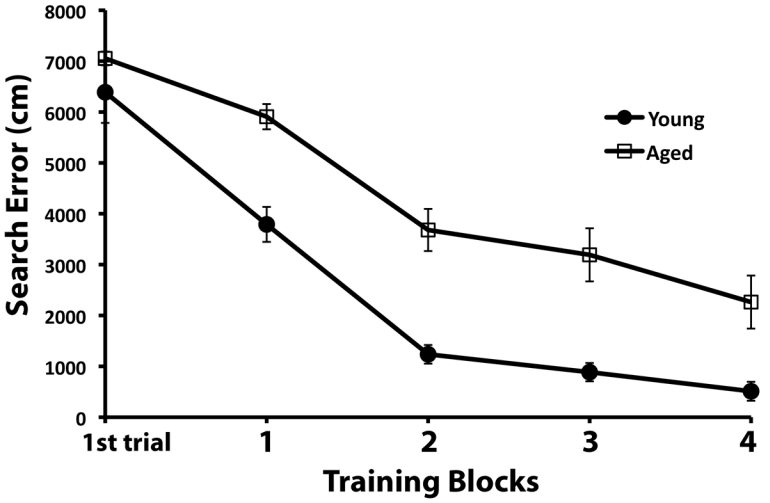

Haberman et al, Figure S2

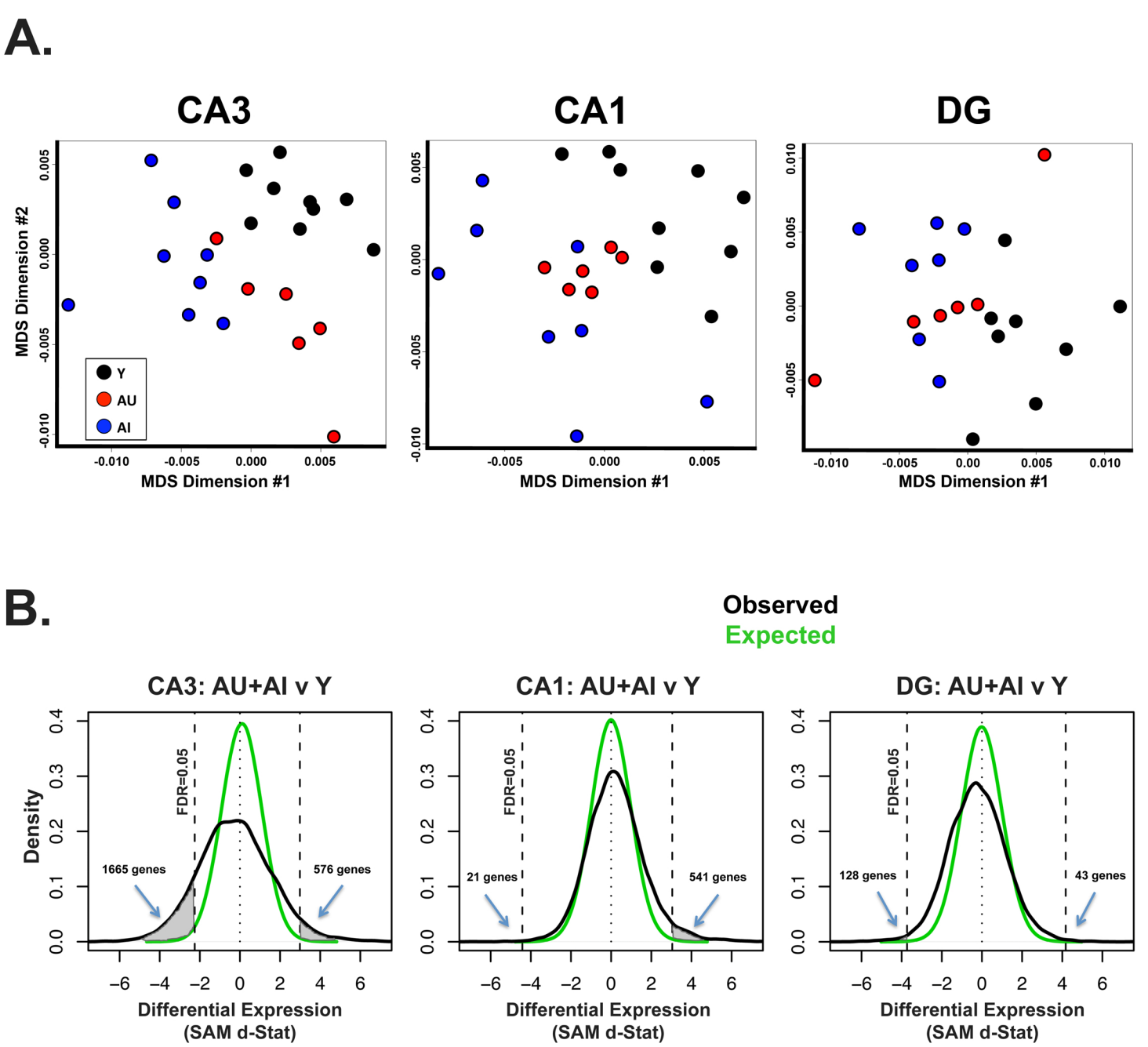

Figure S3

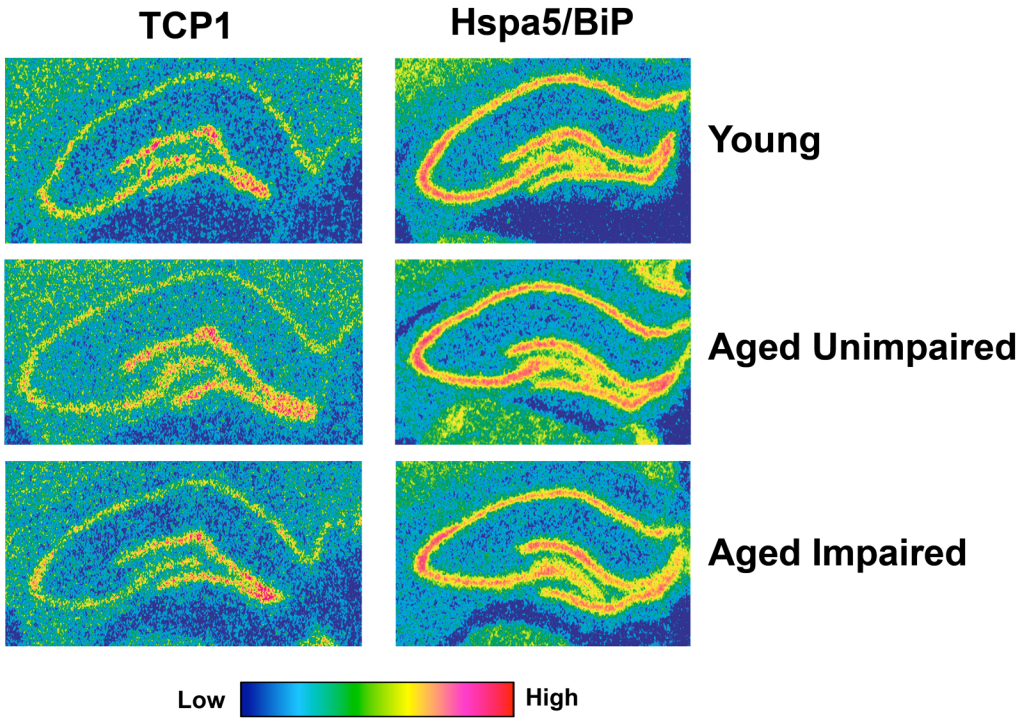
TCP1
Hspa5/BiP
Young
Aged Unimpaired
Aged Impaired
Low
High

Figure S4